USGS
science for a changing world

A Simple Calculator of Ballistic Trajectories for Blocks Ejected during Volcanic Eruptions

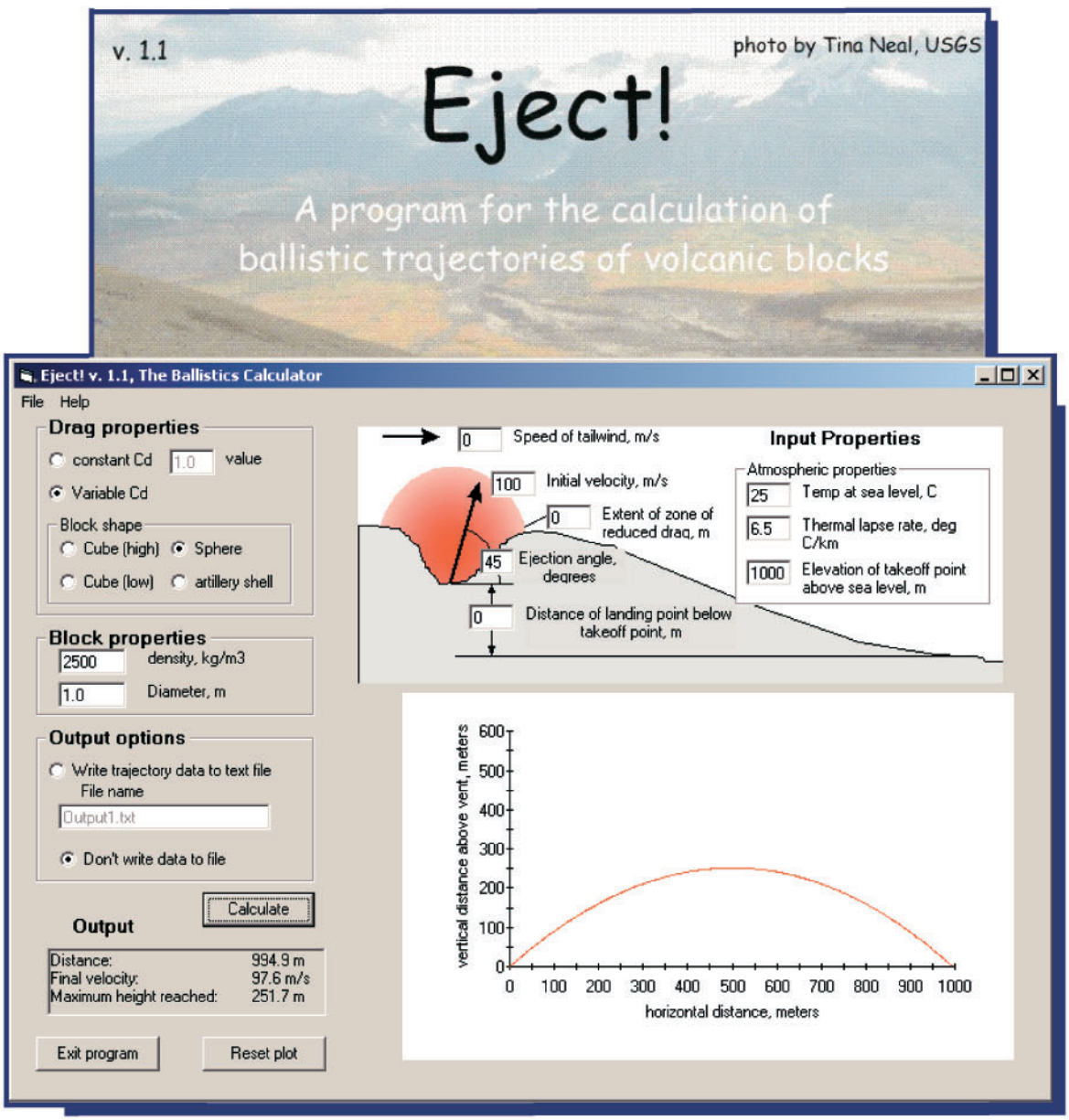

U.S. Geological Survey Open-File Report 01-45, Version 1.2*

*This version number may not correspond to the latest version of the software.

U.S. Department of the Interior
U.S. Geological Survey

U.S. Department of the Interior
Gale A. Norton, *Secretary*

U.S. GEOLOGICAL SURVEY
Charles G. Groat, *Director*

Any use of trade, product, or firm names in this publication is for descriptive purposes only and does not imply endorsement by the U.S. Government

For additional information write to:

U.S. Geological Survey
Cascades Volcano Observatory
1300 SE Cardinal Court, Bldg. 10, Suite 100
Vancouver, Washington 98683-9589

Copies of this report can be purchased from:

U.S. Geological Survey
Information Services
Building 810
Box 25286, Federal Center
Denver, CO 80225-0286

This report is also available in digital form on the World Wide Web.
URL: **http://vulcan.wr.usgs.gov/Projects/Mastin**

Table of Contents

Introduction 1

Method 2

Governing Equations 3

Calculating terms in the governing equations 4

Drag 4

Reduced drag near vent 5

Numerical solution 8

Model validation 8

Special case of zero air drag 8

Comparison with other ballistics calculations 9

Comparison with analytical solution for constant drag coefficient and air density 10

Using Eject! 11

References 12

Figures

1. Photograph showing eruption through a crater lake at Ruapehu Volcano, New Zealand 2
2. Illustration of the forces acting on a block ejected ballistically from a volcanic event 3
3. Graphs showing (*A*) log drag coefficient (C_d) for spheres as a function of log Reynolds number, at low Mach number, and (*B*) drag coefficient for spheres in air at varying Mach numbers 6
4. Graphs showing (*A*) drag coefficient for cubes as a function of Mach number, and (*B*) drag coefficient as a function of Mach number for cylinders, spheres, and the Ingalls-Mayevski ogive-cylinder 7
5. Graph showing the comparison of analytical versus numerical calculations of ballistic trajectories under two sets of conditions described in the text 9
6. Screen capture of graphical user interface for the program Eject! 11

Table

1. Table showing comparison of results calculated by Eject! with those from Miller (1979) for spheres 1.184 cm in diameter ejected with an initial velocity of 579 m/s at an angle of 0.8080 degrees above horizontal into air having a temperature of 15.3°C and a pressure of 1 atmosphere 10

Governing Equations

Blocks in flight are subjected to forces (F) of drag against the ambient fluid, and of gravity. The acceleration of the block (dv/dt) in the horizontal (x) and vertical (z) directions results from those forces (fig. 2):

$$\frac{dv_x}{dt} = \frac{F_x}{m} = \frac{-v_x \rho_a v A C_d}{2m} \qquad \textbf{(1a)}$$

$$\frac{dv_z}{dt} = \frac{F_z}{m} = \frac{-v_z \rho_a v A C_d}{2m} - g\frac{\rho_r - \rho_a}{\rho_r} \qquad \textbf{(1b)}$$

where ρ_a is air density, ρ_r is density of the ballistic block, A is cross-sectional area of the block, C_d is drag coefficient on the block, m is the block's mass, g is gravitational acceleration (9.81 m/s^2), v is the block's velocity (i.e., the magnitude of the velocity vector) and t is time. The first term on the right-hand side of both equations is the force (per unit mass) of air drag. The second term on the right-hand side in equation ***1b*** represents the gravitational force of the block per unit mass. The effect of a horizontal tailwind of velocity w on block motion can be accommodated by replacing v_x with (v_x-w) in ***1a***, and v with $\sqrt{v_z^2 + (v_x - w)^2}$ in ***1a*** and ***1b***.

Equations ***1a*** and ***1b*** ignore the force associated with block rotation, known as the Magnus force, which is responsible for curve balls in baseball and (in part) for the stability of rifle-propelled bullets. In some cases the Magnus force may influence the trajectories of volcanically ejected blocks (Waitt and others, 1995). **Eject!** also ignores cross-wind forces, lift, variations in the gravitational-force vector with position, and the Coriolis force (the latter two are considered in long-range military ballistics calculations).

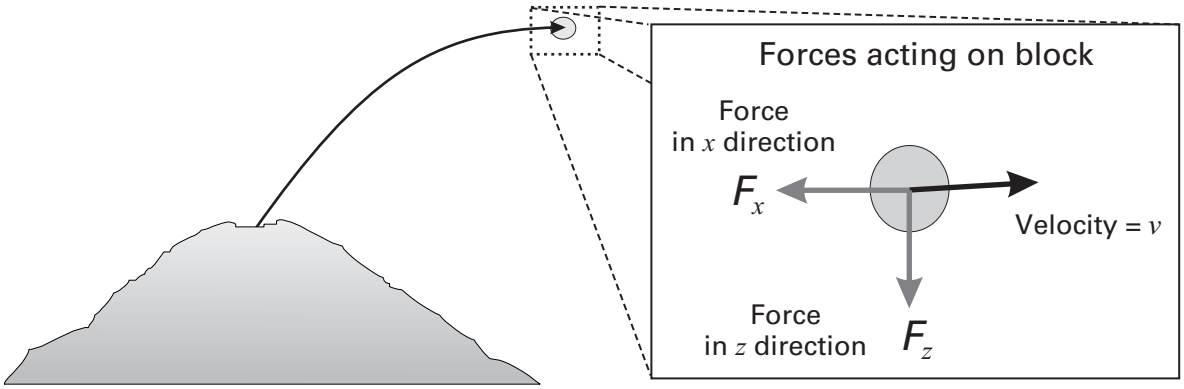

Figure 2. Illustration of the forces acting on a block ejected ballistically from a volcanic vent.

Calculating terms in the governing equations

The parameters in (1) are calculated as follows:

1. A and m depend on the shape and size of the block: $A = D^2$ for cubes in which one face is perpendicular to the flow direction, (where D=block dimension), $\sqrt{3}\,D^2$ for cubes oriented with a corner at the leading edge (1/4) πD^2 for spheres (where D=block diameter), $m = \rho_r D^3$ for cubes, (1/6) $\rho_r \pi D^3$ for spheres.
2. The air density (ρ_a) varies with elevation and is recalculated at each point in the trajectory using the equation for a perfect gas:

$$\rho_a = \frac{p}{RT} \qquad (2)$$

where T is in Kelvin, R is the gas constant for air (286.98 J/(kg K)), and p is the atmospheric pressure in Pascals. The pressure at a given elevation is calculated using the formula:

$$p = p_o \left(\frac{T}{T_o}\right)^{-g/(R(dT/dz))} \qquad (3)$$

where p_o and T_o are the pressure (Pa) and temperature (Kelvin) at sea level and (dT/dz) is the thermal lapse rate in degrees Kelvin per meter[1]. Equation ***3*** is obtained by integrating the equation:

$$\frac{dp}{dz} = -\rho_a g = \frac{-p}{RT}\, g = \frac{-p}{R(T_o + (dT/dz)z)}\, g \qquad (4)$$

The pressure at sea level is assumed to be normal atmospheric, 1.013×10^5 Pa. Values of T_o and (dT/dz) are given as input to the program.

Drag

The drag coefficient (C_d) is the drag force acting on a block, divided by the product of kinetic energy per unit volume of ambient fluid impinging on block and the block's cross-sectional area. The drag coefficient influences the final range of a block but varies greatly depending on its shape, orientation, and roughness. Experimental results (for example, Hoerner, 1965) indicate that C_d for variously shaped objects varies with two dimensionless parameters: Reynolds number (Re) and Mach number (M). The Reynolds number for external flow ($Re \equiv \rho_a v D/\eta$, where η is fluid viscosity) relates the importance of viscous forces (in the denominator) to inertial forces (in the numerator). **Eject!** calculates the Reynolds number from density calculations (described above), specified input values of block diameter, velocity calculated by solution of equation ***1***, and gas viscosity, calculated from the empirical relation for air:

---

[1] Because z increases upward, dT/dz should be negative if temperatures decrease with increasing altitude. This convention is assumed in equation ***3***. However **Eject!** assumes that positive values of thermal lapse rate, entered into the text box in program interface, imply decreasing temperature with elevation. Such values are converted to negative values within the code.

$$\eta = 0.0000172\left(\frac{390}{T+117}\right)\left(\frac{T}{273}\right)^{1.5} \qquad (5)$$

where T is temperature in Kelvin, and viscosity is given in Pascal-seconds.

The value of C_d has been determined experimentally for a variety of shapes; (e.g., for spheres, fig. 3*A*). For blocks ejected during volcanic eruptions, Reynolds numbers almost always exceed ~$1x10^3$. For spheres at Re>~200, C_d is either nearly constant at ~0.5 (fig. 3*A*) or, at Re>~$2x10^5$, drops abruptly to about 0.1. The abrupt drop is associated with a shift in the boundary-layer separation point from a location upstream of the equator of the sphere to a point downstream of the equator. The Reynolds number at which C_d drops differs for differing block shape and block roughness; for spheres, **Eject!** assumes that C_d =~0.5 for 200<Re<$2x10^5$, and ~0.1 for Re>$2x10^5$. For cubes, **Eject!** does not consider reduced values of C_d because the Reynolds number at which boundary-layer separation occurs is so variable.

The relations above govern the drag coefficient so long as the Mach number of the block is less than about 0.5 (~175 m/s for air at T=25°C, p=1 atm). At higher Mach numbers, the drag coefficient increases as pressure waves accumulate ahead of the block. At M= ~1-2, pressure waves coalesce to a single shock wave and drag coefficients reach a maximum. At Mach numbers a few times greater than 1, C_d decreases as the shock front begins to wrap around the object.

Eject! calculates the Mach number ($M \equiv v/c$, where v=velocity and c=sound speed in air) using the relation for sound speed in a perfect gas:

$$c = \sqrt{\gamma RT} \qquad (6)$$

where γ is the ratio of specific heats (C_p/C_v) at constant pressure and constant volume (γ= 1.4 for air). Using values of C_d versus M digitized from figures. 3*B*, 4*A*, and 4*B* for spheres and cubes, **Eject!** uses a cubic spline interpolation routine (Press and others, 1992, p. 101) to determine the drag coefficient for a given Mach number at M>0.5.

Reduced drag near vent

Prior to the early 1990's, investigators assumed that blocks were ejected into still, ambient air from the moment they left the vent. In fact, visual observations (e.g., fig. 1) indicate that the blocks are initially enveloped in a cloud of tephra and other fragments that move at roughly the same velocity as the large blocks and therefore provide little or no drag (and may even provide some lift). The degree to which such drag is reduced and the distance over which drag is less than that in ambient air are not well constrained. Fagents and Wilson (1993) postulate that the ejected mass accelerates to a maximum velocity (v_o) at some distance (r_o) and time (t_o) from its initial position, then decelerates at the rate:

$$v = v_o\left(\frac{r_o}{r}\right)^2 e^{-t/\tau} \qquad (7)$$

where the time constant t is related to the ratio of initial gas pressure (p_{gz}) to atmospheric pressure (p_a):

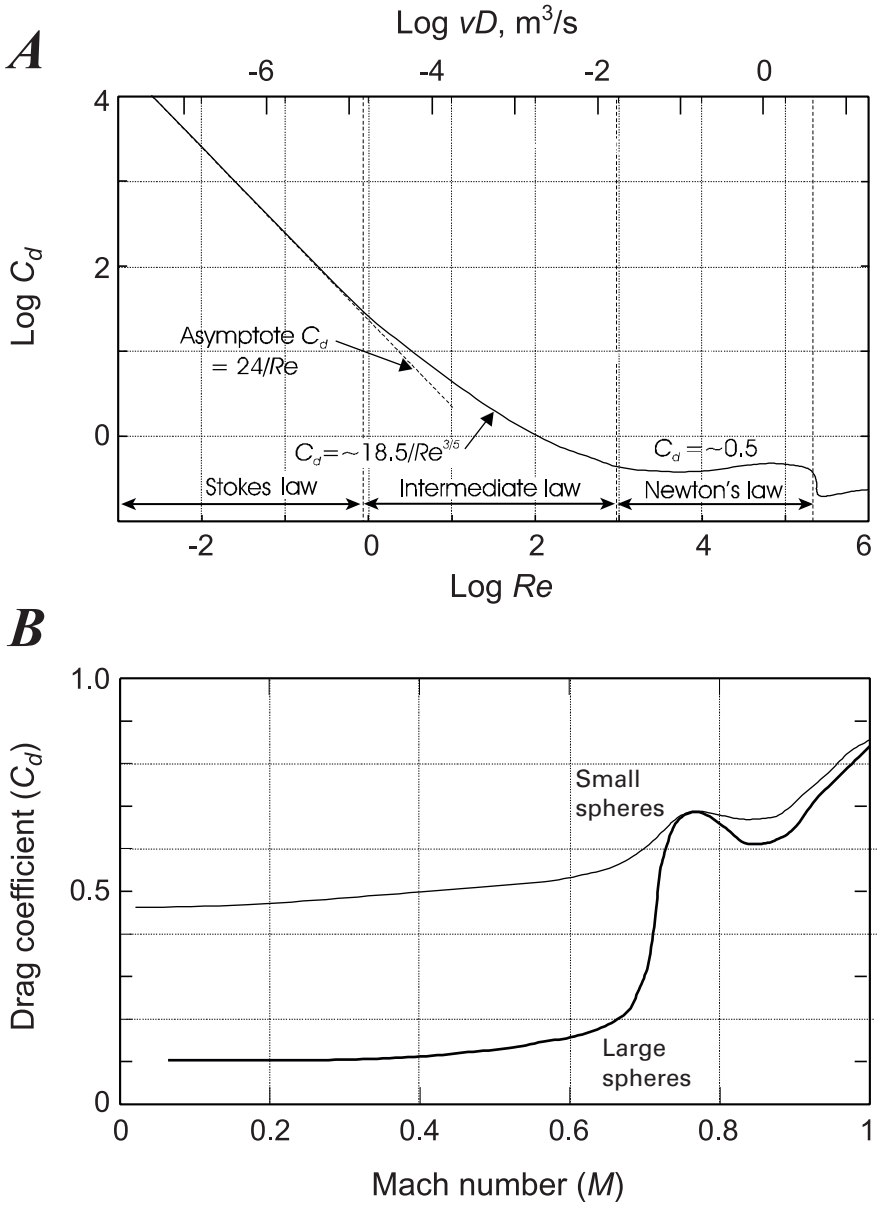

Figure 3. (***A***) Log drag coefficient (C_d) for spheres as a function of log Reynolds number, at low Mach number (from Bird and others, 1960, p. 192). Tick marks at top of plot give the product of velocity (v) times diameter (D) for spheres traveling in a fluid with the viscosity (1.8e-5 Pa s) and density (1.18 kg/m^3) of air at 25^o C, 1 atm pressure. (***B***) Drag coefficient for spheres in air at varying Mach numbers (from Hoerner, 1965). Top curve represents drag coefficients for spheres at Reynolds numbers below the critical transition (Re = ~2x10^5) shown in figure 3*A*, whereas the lower curve represents drag coefficients for large spheres at Re above that transition.

$$\tau = \frac{p_{gz}}{p_a} t_o \qquad (8)$$

The model **Eject!** does not estimate initial gas pressures because relations between initial pressure and velocity tend to be non-unique (they depend, for example, on initial temperature, mass fraction gas in the erupting mixture, the degree to which external water is involved, and the efficiency of conversion of gas enthalpy to kinetic energy; Wilson, 1980; Mastin, 1995). Instead, **Eject!** allows the user to specify (rather arbitrarily) a distance (r_d) from the vent over which drag is reduced. At a radial distance (r) less than r_d, a reduced drag coefficient (C_{dr}) is calculated from the formula:

$$C_{dr} = C_d \left(\frac{r}{r_d} \right)^2 \qquad (9)$$

The value of r_d is likely to be tens to hundreds of meters, judging from photographs such as that in figure 1 (or those in Nairn and Self, 1978), and assuming that most of the reduced drag exists when the block is enveloped within the tephra cloud. More accurate estimates of r_d, and better relations between C_{dr} and C_d, will require more sophisticated modeling of volcanic explosions than has been accomplished to date.

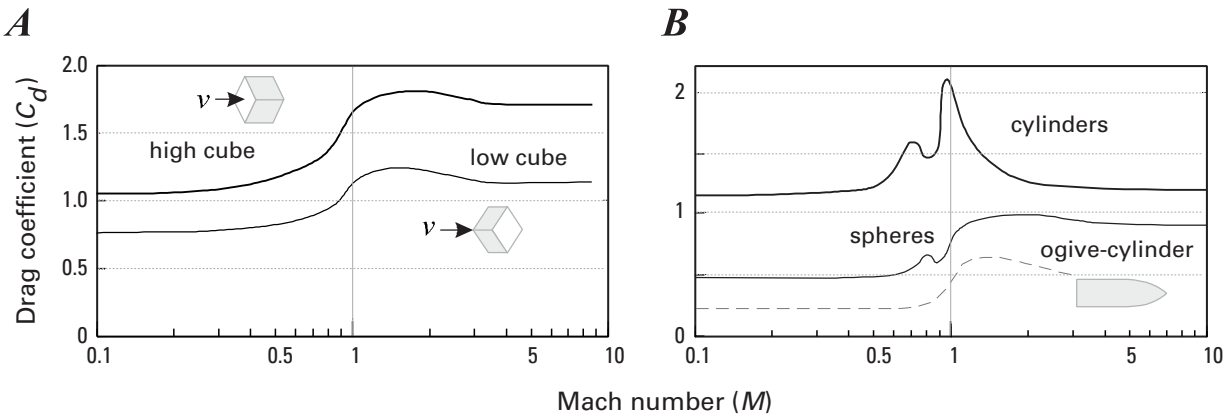

Figure 4. (***A***) Drag coefficient for cubes as a function of Mach number. The drag coefficient varies with orientation of the cube: C_d is highest when one face is oriented perpendicular to the direction of motion, lowest when the vertex between three faces is at the leading edge of the cube. (***B***) Drag coefficient as a function of Mach number for cylinders (top), spheres (middle), and the Ingalls-Mayevski ogive-cylinder (bottom). The last of these three is the shape of a G1 artillery shell for which classic ballistics tables were calculated (e.g., Ingalls, 1886). Figures derived from Hoerner (1965) and Miller (1979).

Numerical solution

Equations ***1a*** aand ***1b*** above are integrated throughout the trajectory using a fourth-order Runge-Kutta method (Press and others, 1992, p. 706). The calculations continue until the vertical position (z) of the block reaches a specified landing elevation (z_f).

MODEL VALIDATION

The verification of numerically calculated ballistic trajectories such as these for blocks during volcanic eruptions has never been attempted. Such a study would help test the simplifying assumptions made in a model such as this one. In lieu of such a study, I compare the calculations made by this model with the special case of $C_d = 0$, for which analytical solutions exist, and with an independent set of ballistics calculations for small spheres (Miller, 1979). I also compare the results of **Eject!** with those for an approximate, analytical solution that assumes constant drag coefficient and constant air density.

Special case of zero air drag

In cases where the air drag is zero and where the density of ambient air is insignificant compared to that of the block, equations ***1a*** and ***1b*** simplify to $dv_x/dt = 0$, and $dv_z/dt = -g$, respectively. Integrating equations ***1a*** and ***1b*** twice with respect to time, the position of the block at a given point in its trajectory is then:

$$x(t) = v_i \cos\theta \, t \qquad \textbf{(10a)}$$

$$z(t) = v_i \sin\theta \, t - \frac{1}{2} \, gt^2 \qquad \textbf{(10b)}$$

where v_i is the initial velocity (i.e., the magnitude of the initial velocity vector). Assuming that the block travels to a landing point whose elevation equals that of the takeoff point, the final distance (x_{final}) reached by the block is:

$$x_{final} = \frac{v_i^2 \sin 2\theta}{\mathrm{g}} \qquad \textbf{(11)}$$

Values of x_{final} calculated using equation ***11*** are compared with those calculated by **Eject!**, assuming $C_d = 0$, in figure 5.

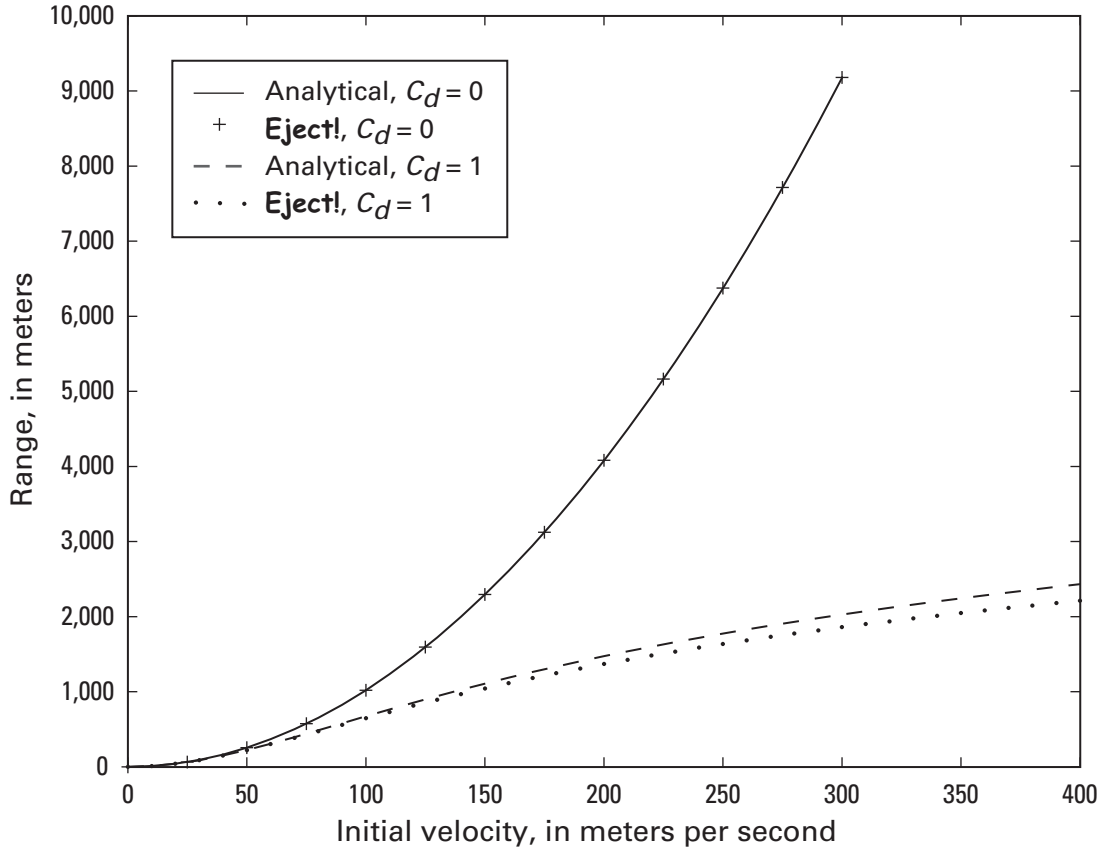

Figure 5. Range (x_{final}) versus initial velocity for a 40-centimeter diameter spherical block, with r_r=2,500 kg/m^3 and q=45°. Solid line gives the analytical solution for C_d= 0; crosses give the range calculated by **Eject!** for the same conditions. Dashed line gives the solution calculated using equations (***13***) and (***14***) for C_d=1; dots give the solution for a constant C_d=1 using **Eject!**

Comparison with other ballistics calculations

Table 1 compares the results of **Eject!** with calculations from Miller (1979) for small spheres. The trajectories of such small clasts are generally not studied by volcanologists because they are so easily influenced by plume currents. On the other hand, their sensitivity to air drag makes them especially appropriate for a test of the numerical solution procedure used here. Miller conducted a set of experiments on drag of small spheres and used their results in a refined ballistics table for such spheres. Miller's calculations use the Sciacci approximation, which is used in classical ballistics tables (e.g., Ingalls, 1886, Hermann, 1930). The Sciacci approximation assumes that, for projectiles ejected in a near-horizontal trajectory, the term cosθ can be replaced with a constant, making the integration simpler. No such approximation is used by **Eject!** The results of Miller's calculations differ from those of **Eject!** primarily in the third significant figure.

Table 1. Comparison of results calculated by Eject! (right three columns) with those from Miller (1979, table 2) for spheres 1.184 cm in diameter ejected with an initial velocity of 579 m/s at an angle of 0.8080 degrees above horizontal into air having a temperature of 15.3°C and a pressure of 1 atmosphere. The results give the final distance traveled (x_f), final velocity on impact (v_f), and time of flight (t_f).

		From Miller (1979)			From **Eject!**		
Material	Density (kg/m^3)	x_f(m)	v_f(m/s)	t_f(sec)	x_f(m)	v_f(m/s)	t_f(sec)
pumice	700	45.63	37.09	0.456	48.59	37.34	0.476
Mg	1,740	87.63	61.78	0.638	86.90	59.77	0.64
basalt	2,700	117.90	78.70	0.737	117.20	77.11	0.728
steel	8,920	224.70	136.18	0.961	223.88	136.09	0.96
Pb	11,340	274.32	161.82	1.046	273.41	161.76	1.047
W	18,800	352.50	200.22	1.164	351.40	199.74	1.164

Comparison with analytical solution for constant drag coefficient and air density

In cases where the drag coefficient and air density are constant, analytical solutions for block trajectory and for the range traveled by blocks exist (Minakami, 1942; Self and others, 1980; Mastin, 1991). However in order to integrate equations ***1a*** and ***1b***, the product $v_x v$ in (***1a***) must be replaced with $v_x^2 \mathrm{sgn}(v_x)$, and, in ***1b***, $v_z v$ must be replaced with $v_z^2 \mathrm{sgn}(v_z)$, where "sgn" refers to the sign of these terms. This simplification results in underestimating the drag force along the trajectory by the factor $(\sin^4\theta + \cos^4\theta)^{1/2}$ (Sherwood, 1967). The resulting equations are:

$$\frac{dv_x}{dt} = \frac{-\rho_a C_d A v_x^2 \ \mathrm{sgn}(v_x)}{2m} \qquad \textbf{(12a)}$$

$$\frac{dv_z}{dt} = \frac{-\rho_a C_d A v_z^2 \ \mathrm{sgn}(v_z)}{2m} - g \qquad \textbf{(12b)}$$

Equation ***12a*** can be integrated twice to give the range of flight (x_{final}) of a block whose landing elevation equals its takeoff elevation:

$$x_{final} = \frac{1}{\mu} \ln(\mu v_i \cos\theta \, t_f + 1) \qquad \textbf{(13)}$$

where $\mu = (r_a C_d A)/2m$ and t_f is the total time of travel of the block. The value of t_f is obtained by evaluating the integral of ***12b*** to obtain the time of flight from the initial point ($v_z = v_i \sin\theta$) to the top of the trajectory ($v_z = 0$), then integrating again to determine the time of flight from the top of the trajectory to the landing elevation ($z = 0$).

$$t_f = \frac{1}{\sqrt{\mu g}} \left[\cosh^{-1} \sqrt{1 + \frac{\mu}{g} v_i^2 \sin^2\theta} + \tan^{-1} \left(\sqrt{\frac{\mu}{g}} v_i \sin\theta \right) \right] \qquad \textit{(14)}$$

The analytical solution for the flight distance as a function of initial velocity is compared with results from Eject! in figure 5 for blocks 40 cm in diameter, with $\rho_r = 2500$ kg/m^3, $\theta = 45°$. The analytical and numerical solutions agree at low initial velocity (v_i <~150 m/s), where drag is unimportant, and differ at higher velocities. The discrepancy between analytical and numerical solutions increases as block diameter decreases.

Using Eject!

The program Eject! , along with this documentation, can be downloaded from the web site http://vulcan.wr.usgs.gov/Projects/Mastin. The program can operate on any Windows®-based personal computer running Windows 95 or later, and containing at least 3 megabytes of hard disk space. To install the program, do the following:

1) Save the self-extracting Zip® file, "ejectzip_2.exe" to your hard drive,
2) Double-click on the file icon. It will expand into three files and place them in a new folder entitled "Eject 1.1."
3) Go into the new folder and double-click on the icon "setup.exe." Follow the instructions on the screen to install the program.
4) Go to the Start button, then to Programs, then choose the icon "eject" to launch the program.

Launching the program will display an introductory screen, followed (after clicking on the screen) by the window shown in figure 6. The box in the upper right hand corner gives specified input conditions for block velocity, ejection angle, tailwind velocity, and vertical distance of landing point below takeoff point. Also included are the elevation of the takeoff point, the atmospheric temperature at the vent, and the thermal lapse rate, all of which are used to calculate air density, pressure, and sound speed as a function of elevation during the block's trajectory.

The input conditions, and calculations of the block's trajectory during flight, may be written to a file whose name is specified in the "output options" box. If only a file name is given (excluding a full path name), the file will be written to the same directory that contains the program Eject! (usually "c:\program files\eject").

The current version at the time of writing of this report (version 1.1.0) corrects errors in calculating the mass and frontal area of cubes, which were present in version 1.0.0. Unlike version 1.0.0, version 1.1.0 keeps radio buttons for block shape enabled when the "constant *Cd*" radio button is chosen.

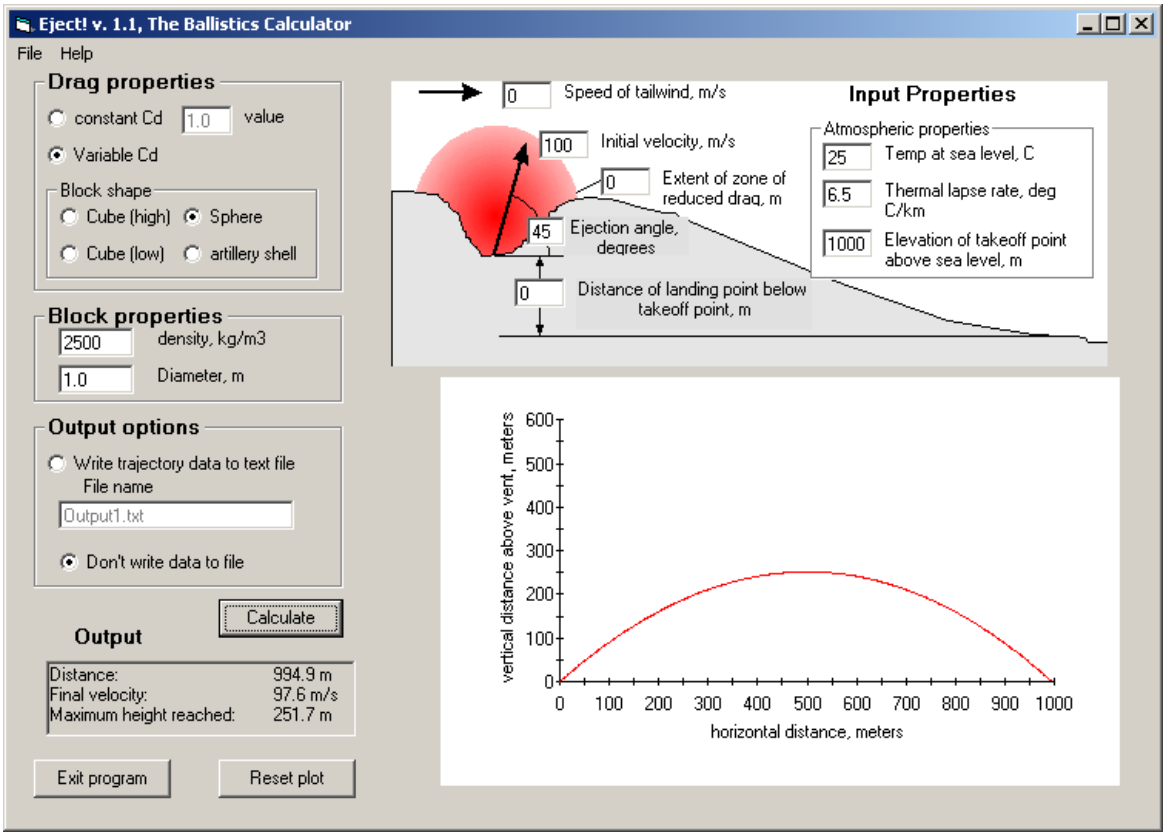

Figure 6. Graphical user interface for the program **Eject!**

REFERENCES

Bird, R.B., Stewart, W.E., and Lightfoot, E.N., 1960, Transport phenomena: New York, John Wiley and Sons, 780 p.

Fagents, S.A., and Wilson, L., 1993, Explosive volcanic eruptions; VII, The ranges of pyroclasts ejected in transient volcanic explosions: Geophysical Journal International, v. 113, no. 2, p. 359-370.

Gorshkov, G.S., 1959, Gigantic eruption of the Volcano Bezymianny: Bulletin Volcanologique, v. 21, p. 77-109.

Hermann, E.E., 1930, Exterior ballistics: Annapolis, MD, U.S. Naval Institute, 354 p.

Hoerner, S.F., 1965, Fluid dynamic drag; Practical information on aerodynamic drag and hydrodynamic resistance: Vancouver, WA, published by the author, 440 p.

Ingalls, J.M., 1886, Exterior ballistics in the plane of fire: New York, D. Van Nostrand, 173 p.

Mastin, L.G., 1991, The roles of magma and groundwater in the phreatic eruptions at Inyo Craters, Long Valley Caldera, California: Bulletin of Volcanology, v. 53, p. 579-596.

———, 1995, Thermodynamics of gas and steam-blast eruptions: Bulletin of Volcanology, v. 57, no. 2, p. 85-98.

Miller, D.G., 1979, Ballistics tables for spheres 7.5 to 25 mm (0.3 to 1 in.) in diameter: Lawrence Livermore Laboratory Report UCRL-52755. Livermore, Calif.: Dept. of Energy, Lawrence Livermore Laboratory, 89 p.

Miller, D.G., and Bailey, A.B., 1979, Sphere drag at Mach numbers from 0.3 to 2.0 at Reynolds numbers approaching 10^7: Journal of Fluid Mechanics, v. 92, p. 449-464.

Minakami, T., 1942, On the distribution of volcanic ejecta (Part I). The distributions of volcanic bombs ejected by the recent explosions of Asama: Bulletin of the Earthquake Research Institute, Tokyo, v. 20, p. 65-91.

Nairn, I.A., and Self, S., 1978, Explosive eruptions and pyroclastic avalanches from Ngauruhoe in February 1975: Journal of Volcanology and Geothermal Research, v. 3, p. 39-60.

Press, W.H., Vetterling, W.T., Teukolsky, S.A., and Flannery, B.P., 1992, Numerical recipes (2nd ed.): Cambridge, Cambridge University Press, 933 p.

Self, S., Kienle, J., and Huot, J.-P., 1980, Ukinrek Maars, Alaska, II. Deposits and formation of the 1977 craters: Journal of Volcanology and Geothermal Research, v. 7, p. 39-65.

Sherwood, A.E., 1967, Effect of air drag on particles ejected during explosive cratering: Journal of Geophysical Research, v. 72, no. 6, p. 1783-1791.

Waitt, R.B., Mastin, L.G., and Miller, T.P., 1995, Ballistic showers during Crater Peak eruptions of Mount Spurr Volcano, Summer 1992, *in* Keith, T.E.C., ed., The 1992 eruptions of Crater Peak Vent, Mount Spurr Volcano, Alaska: U.S. Geological Survey Bulletin 2139: Washington D.C., U.S. Geological Survey, p. 89-106.

Wilson, L., 1972, Explosive volcanic eruptions—II. The atmospheric trajectories of pyroclasts: Geophysical Journal of the Royal Astronomical Society, v. 30, p. 381-392.

———, 1980, Relationships between pressure, volatile content and ejecta velocity in three types of volcanic explosion: Journal of Volcanology and Geothermal Research, v. 8, p. 297-313.